# Studies of human, mouse and yeast homologues indicate a mitochondrial function for frataxin

Hana Koutnikova[1], Victoria Campuzano[1], Françoise Foury[2], Pascal Dollé[1], Ornella Cazzalini[2] & Michel Koenig[1]

**Friedreich's ataxia is due to loss of function mutations in the gene encoding frataxin (FRDA). Frataxin is a protein of unknown function. *In situ* hybridization analyses revealed that mouse frataxin expression correlates well with the main site of neurodegeneration, but the expression pattern is broader than expected from the pathology of the disease. Frataxin mRNA is predominantly expressed in tissues with a high metabolic rate, including liver, kidney, brown fat and heart. We found that mouse and yeast frataxin homologues contain a potential mitochondrial targeting sequence in their N-terminal domains and that disruption of the yeast gene results in mitochondrial dysfunction. Finally, tagging experiments demonstrate that human frataxin co-localizes with a mitochondrial protein. Friedreich's ataxia is therefore a mitochondrial disease caused by a mutation in the nuclear genome.**

Friedreich's ataxia (FRDA) is an autosomal recessive neurodegenerative disease with an estimated incidence of 1 in 50,000 (refs 1,2). It is characterized by progressive gait and limb ataxia, hypertrophic cardiomyopathy and increased incidence of diabetes mellitus[3,4]. The onset of symptoms usually occurs at about the time of puberty, and typically before the age of 25. Most patients are wheelchair-bound in the third decade of life.

FRDA primarily affects the central and peripheral nervous systems and heart. The first pathological changes occur in the dorsal root ganglia, with the loss of large sensory neurons, followed by neuron degeneration in Clarke's and posterior columns and pyramidal and dorsal spinocerebellar tracts of the spinal cord[5]. Mild degenerative changes are also observed in the medulla, cerebellum and pons.

FRDA is caused primarily by an unstable GAA repeat expansion within the first intron of the *FRDA* gene that accounts for 98% of mutant alleles[6]. A few patients are compound heterozygotes for a nonsense or splice mutation and expansion, indicating that the latter mutation also leads to loss of function, most likely by lowering *FRDA* mRNA abundance[6,7]. The encoded protein, frataxin, is predicted to be a 210–amino acid protein with highly significant sequence identity (49% and 31%, respectively) to proteins of unknown function in *Caenorhabditis elegans* and *Saccharomyces cerevisiae*[6] and, to a lesser extent, to proteins in gram-negative bacteria[8]. The recent suggestion that the frataxin gene and the neighbouring *STM7* gene[9] are part of the same transcription unit is based on indirect evidence that contradicts observations concerning the structure of cDNAs isolated from conventional cDNA libraries and the finding of point mutations in *FRDA*[6,7], but not in *STM7* (ref. 10).

Little is known about frataxin expression and function. In the present work, we cloned the complete coding region of mouse frataxin cDNA and investigated its pattern of expression in developing and adult tissues. Because the N-terminal sequence of mouse and yeast frataxins revealed a potential mitochondrial targeting signal, we investigated both the subcellular localization of human frataxin by tagging experiments, and the yeast phenotype resulting from gene-targeted disruption.

## Analysis of the mouse frataxin transcript

Murine frataxin cDNAs were cloned by screening a 10.5-day-old embryo cDNA library, using human *FRDA* as a probe. The obtained clones—*mf1*, *mf2* and *mf3*—overlap and encompass the complete mouse frataxin coding sequence (Fig. 1*a*; Genbank accession number U95736). The first in-frame ATG codon corresponds to the postulated initiation codon found in *FRDA*. The mouse gene (*Frda*), is predicted to encode a 207–amino acid protein showing 73% amino acid identity to its human counterpart, with low conservation over the first two exons (Fig. 1*b*). The N-terminal region of mouse frataxin is predicted by the PSORT program[11] to contain a mitochondrial targeting sequence with a positive score of 1.95 (the corresponding score for the human protein is 0.58) and an overall probability of 0.6 to localize to the mitochondria. The independent search of mitochondrial targeting signal in open reading frames identified during the systematic sequencing of the yeast genome[12] revealed that the N-terminal sequence of Yd1120w (Fig. 1*b*), which corresponds to the yeast frataxin homologue (YFH1), has a mitochondrial targeting discriminating score of 4.95 and is predicted to localize to the mitochondria with a probability of 0.9. No other possible localization is predicted.

The expression pattern of the *Frda* gene in adult tissues was studied by northern blot analysis. A major transcript of 1.2 kb, similar in size to the human one, was detected in adult heart, liver, skeletal muscle, kidney, spleen and thymus and, much more weakly, in brain and lung (Fig. 2).

To test whether the faint signal on northern blots of brain tissue corresponds to region-specific expression, we analysed adult brain sections by *in situ* hybridization. Specific labelling was seen at the level of the lateral ventricles, within both the choroid plexus and the ependymal cell layer (Fig. 3*c*). Signals above background were

[1]*Institut de Génétique et Biologie Moléculaire et Cellulaire (IGBMC), INSERM, CNRS, Université Louis Pasteur, 1 rue Laurent Fries, BP 163, 67404 Illkirch Cedex-Strasbourg, France.* [2]*Unité de Biochimie Physiologique, Université Catholique de Louvain, Place Croix du Sud 2/20, B-1348 Louvain-la Neuve, Belgium. H.K. and V.C. contributed equally to this work. Correspondence should be addressed to M.K. e-mail: mkoenig@igbmc.u-strasbg.fr*

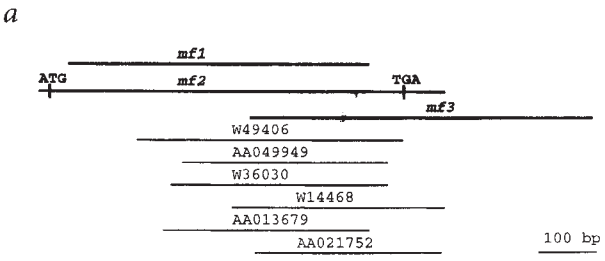


b

```
                1                                                  50
mouse     MWAFGGRAAV GLLPRTAS.R ASAWVGNPRW REPIVTCGRR GLHVTVNAGA
human     MWTLGRRAVA GLLASPSPAQ AQTLTRVPRP AELAPLCGRR GLRTDIDATC
yeast        MIKRSLA SLV.RVSSVM GRRYMIAAAG GERARFCPAV TNKKNHTVNT

               51                                                 100
mouse     T.RHAHLNLH YL.QILNIKK QSVCVVHLRN LGTLDNPSSL DETAYERLAE
human     TPRRASSNQR GLNQIWNVKK QSVYLMNLRK SGTLGHPGSL DETTYERLAE
yeast     FQKRFVESST DG..... QVVPQEVLN. .........L PLEKYHEEAD

              101                                                 150
mouse     ETLDSLAEFF EDLADKPYTL EDYDVSFGDG VLTIKLGGDL GTYVINKQTP
human     ETLDSLAEFF EDLADKPYTF EDYDVSFGSG VLTVKLGGDL GTYVINKQTP
yeast     DYLDHLLDSL EELSEAHP.D CIPDVELSHG VMTLEIP.AF GTYVINKQPP

              151                                                 200
mouse     NKQIWLSSPS SGPKRYDWTG KNWVYSHDGV SLHELLAREL TKALNTKLDL
human     NKQIWLSSPS SGPKRYDWTG KNWVYSHDGV SLHELLAAEL TKALKTKLDL
yeast     NKQIWLASPL SGPNRFDLLN GEWVSLRNGT KLTDILTEEV EKAISKSQ

              201
mouse     SSLAYSGKGT
human     SSLAYSGKDA
```

also observed in the Purkinje cell layer and granule cell layer of the cerebellum. However, the labelling of the Purkinje cells may not be specific, as similar signals were obtained in this layer with the sense control probe (Fig. 3*d*).

### *Frda* expression in embryos and newborns

In order to analyse the developmental pattern of frataxin expression, we performed *in situ* hybridization on sections of mouse embryos, fetuses and young animals. We performed both transverse and sagittal sections at embryonic days 8.5 to 18.5 and transverse sections on young animals at post-natal days 7 and 14.

*Frda* transcripts appeared to be spatially restricted in the developing nervous system and signal was restricted to the ventricular zone of the brain at the level of the telencephalon, including cerebral cortex and the ganglionic eminence, and of the posterior mesencephalon (Fig. 4*a*). Expression in the ventricular zone, which corresponds to dividing neuronal precursors, was seen to start at day 12.5, increase during embryonic development and persist at post-natal day 7 (P7) in the ependymal layer, which is the remnant of the ventricular zone. Weak signals were seen in the spinal cord and medulla oblongata, starting at embryonic day 14.5 (E14.5, Fig. 4*a*), but remained at or just above background level (Fig. 3*b*). Expression was observed in dorsal root ganglia, starting at embryonic day 14.5 (E14.5, Fig. 4*a*). At P14, expression in the dorsal root ganglia was restricted to the cortical region (Fig. 3*b*), where the sensory neuron cell bodies are located. However, the use of frozen sections in these experiments prevented the identification of individual cell types. Other parts of the central nervous system appeared negative at these developmental stages. Weak signals were found in the outermost (and possibly innermost) cells of the retina from E12.5 onwards (Fig. 3*a*).

*Frda* was also expressed in specific patterns in non-neural tissues. Strong expression was seen in the developing liver from E10.5 (shown at E14.5, Fig. 4*a*). In addition, expression was detected in the heart and in the cortex of the developing kidney at E12.5 and later (Fig. 4*a*,*c* and data not shown). Very high expression of *Frda* was observed in brown adipose tissue, which contains high numbers of mitochondria. Expression was observed in small islands around the neck and back at E14.5 (Fig. 4*a*), then in larger masses at E16.5 (Fig. 4*b*) and E18.5. Brown adipose tissue expression was absent at P14, as this tissue regresses after birth. Expression was also seen in the thymus and developing gut at E14.5 (Fig. 4*a*) and until post-natal life. At P14, expression in thymus was restricted to the proliferating cells in the cortical zone, while it became apparent in the spleen (data not shown). A signal was detected in the lungs at E14.5 (Fig. 4*a*). Overall, frataxin expression increased during development from E8.5 (not detectable) to E16.5, when it reached a peak in liver, kidney and brown adipose tissue.

### Mitochondrial localization of human frataxin

Both targeting signal prediction and tissue pattern of expression suggest that mouse frataxin is a mitochondrial protein. To test whether human frataxin also contains a mitochondrial targeting sequence, despite low prediction, the human sequence was tagged at the 3′ end with β-galactosidase (β-gal) in a eukaryotic expression vector. When transfected in HeLa cells, the fusion protein appeared to localize in cytoplasmic granules, consistent with mitochondrial localization, while the β-gal protein alone shows a diffuse cytoplasmic staining (Fig. 5 *a*,*b*). Confirmation of the mitochondrial iden-

**Fig. 1** ***a***, Schematic alignment of mouse frataxin cDNA clones, *mf1*, *mf2* and *mf3*, and mouse ESTs. ***b***, Predicted amino acid sequences of the mouse, human and yeast frataxins. Identical amino acid residues are indicated in bold. The amino-terminal region with typical features of a mitochondria-targeting peptide (an amphiphilic α-helix rich in basic and hydroxylated residues and lacking acidic residues)[15] is underlined.

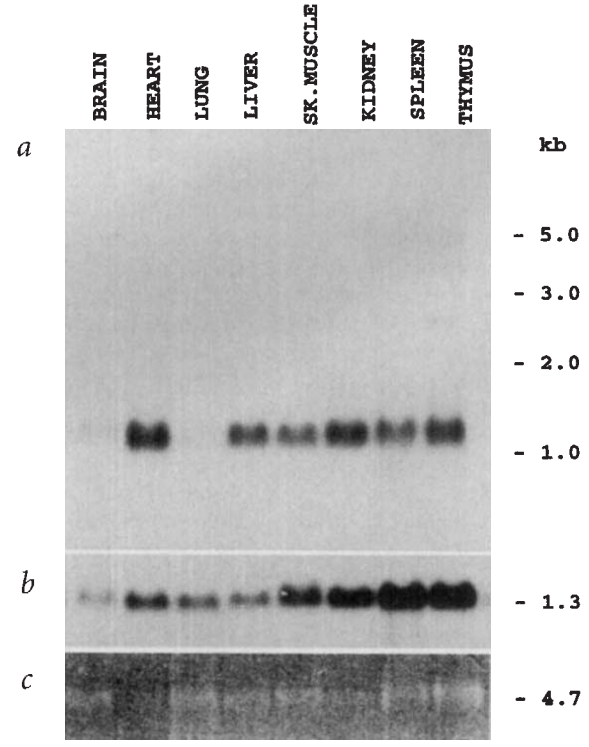


**Fig. 2** Total RNA northern-blot analysis of the mouse frataxin transcript. ***a***, Hybridization with the *mf1* cDNA probe. Tissue is indicated above each lane. ***b***, Hybridization of the same blot with a mouse acidic ribosomal phosphoprotein PO (36B4) probe. ***c***, Ethidium bromide–stained 28S RNA of the corresponding gel, demonstrating that the acidic ribosomal phosphoprotein PO is expressed to a lesser extend in brain compared to other tissues.

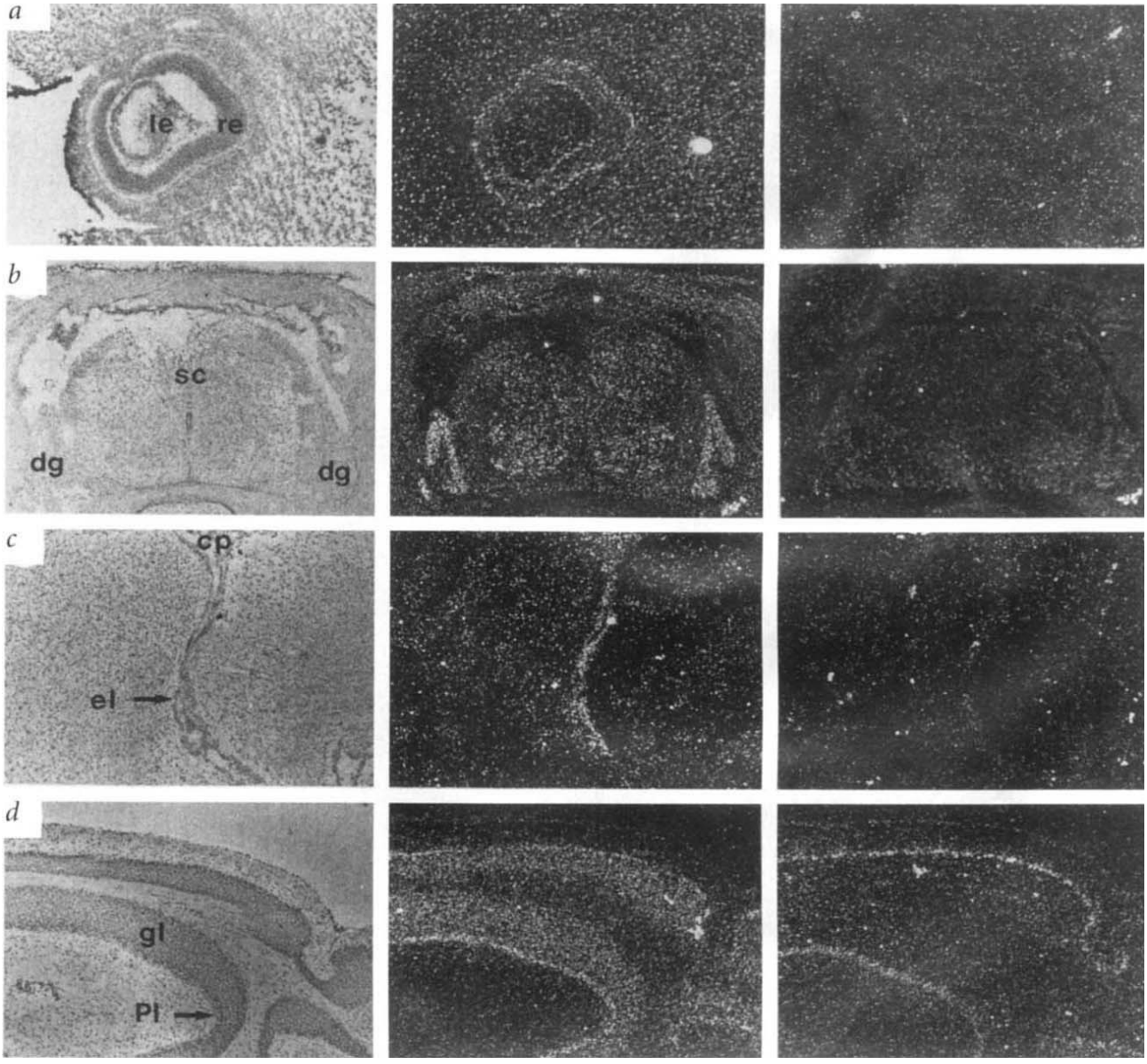


**Fig. 3** *In situ* analysis of *Frda* transcripts in neural tissues. ***a,*** Parasagittal section through the eye of an embryo at E12.5 showing weak labelling in the retina. As in all following figures, the three panels are, from left to right, a bright-field view of the section hybridized with an *mf1* antisense riboprobe, a dark-field view showing the autoradiography signal grains in white and a corresponding dark-field view of the neighbouring section hybridized to the *mf1* sense ('negative control') riboprobe. ***b,*** Post-natal expression of mouse frataxin transcripts in the dorsal root ganglia. Transverse section through the thoracic region of the spinal cord of an animal at post-natal day 14. Transcripts are restricted to the peripheral region of the dorsal root ganglia. The higher background with the anti-sense *versus* sense probes reflects a low level of expression in most tissues, as the sense probe had more radioactivity incorporated than the anti-sense probe. ***c,*** Section of an adult mouse brain at the level of the lateral ventricle and choroid plexus. Note the labelling in the choroid plexus and ependymal layer. ***d,*** Section of an adult mouse cerebellum showing signal in the granule cell layer. Signals in the Purkinje cell layer may not be specific, because similar labelling was obtained in this layer with the sense control probe. cp, choroid plexus; dg, dorsal root ganglia; el, ependymal layer; gl, granular cell layer; le, lens; Pl, Purkinje cell layer; re, retina; sc, spinal cord.

tity of the cytoplasmic granules was obtained by double indirect immuno-cytofluorescence with anti–β-gal and an anti-mitochondrial protein antibody. Identical staining was obtained with both anti–β-gal (stained in green) and anti–cytochrome-c oxidase antibody (stained in red; Fig. 5*b,c*). Co-localization of the two antibodies was demonstrated by the appearance of an intermediate yellow colour (Fig. 5*d*).

## Phenotype after disruption of the yeast frataxin gene

Yeast gene disruption is a rapid means of screening for a metabolic phenotype such as mitochondria-dependent respiration. The yeast frataxin gene, YFH1, was deleted in the haploid strain D273UK by insertion at the homologous site of the selectable $kan^R$ marker. After transformation, more than 50% of the deletant clones (D273ΔYdl120) failed to grow on glycerol, a non-fermentable carbon source, and exhibited a petite phenotype (also shown by $rho^-$ mutants defective in mitochondrial DNA). A glycerol-positive D273ΔYdl120 clone was selected for further analysis of the stability of the mitochondrial genome and respiratory competence. After four to five generations in a glycerol-rich medium (YG), the wild-type and deletant strains were transferred in a glucose-rich medium (YPD) and grown at 28 °C and 37 °C for about ten generations,

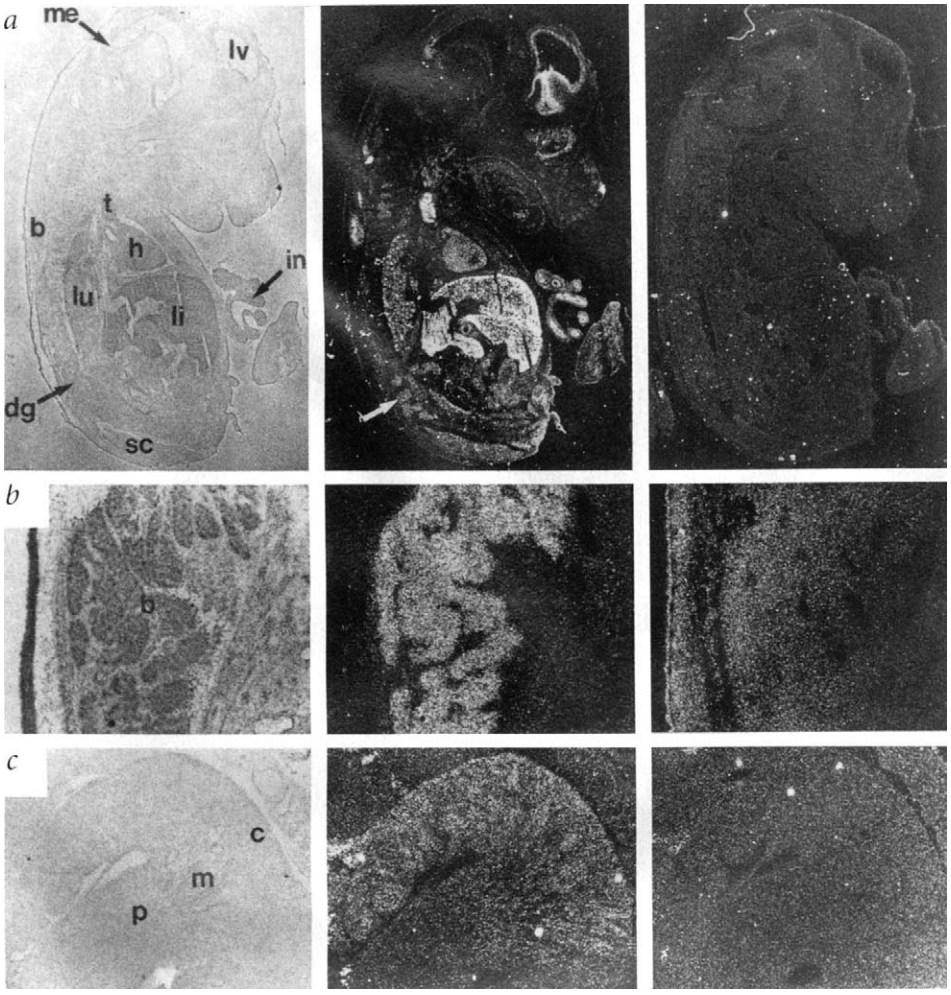


**Fig. 4** *In situ* analysis of mouse frataxin expression during development. ***a,*** Parasagittal sections through an embryo at E14.5. Strong labelling is shown in the ventricular zone of the developing brain (lateral ventricle and ganglionic eminence), brown adipose tissue, liver, intestine and thymus. Weaker labelling is detected in the mesencephalic vesicle, heart, lung, dorsal root ganglia and spinal cord. ***b,*** Expression of mouse frataxin transcripts in the brown adipose tissue. Detail of a sagittal section through an embryo at day 16.5. ***c,*** Post-natal expression of mouse frataxin transcripts in the kidney during development. Transverse section through the lower abdominal region of an animal at post-natal day 7. Frataxin transcripts are detected in the cortical region of the kidney during development. b, brown adipose tissue; c, cortex of kidney; dg, dorsal root ganglia; h, heart; in, intestine; li, liver; lu, lung; lv, lateral ventricle; m, medulla of kidney; me, mesencephalic vesicle; p, papilla of kidney; sc, spinal cord; t, thymus.

after which they were spread on YPD plates and grown at 28 °C. D273ΔYdl120 colonies were scalloped and small compared to wild-type strains (Fig. 6*a*). Replica-plating on YG medium gave rise to sectors, papillae or even total absence of growth, suggesting that many rho$^-$ mutants were produced among cells in individual colonies (Fig. 6*b*). We found that 25% of the D273ΔYdl120 cells grown at 28 °C and 99% of those grown at 37 °C gave rise to rho$^-$ colonies, in contrast with the wild-type strain (Table 1).

The rho$^-$ character of a haploid colony, which does not grow on glycerol, can be determined in a cross with a rho$^0$ tester strain of opposite mating type and wild-type nuclear background. Restoration of the capacity to grow on glycerol in the diploids implies that the glycerol-negative haploid mutant has a wild-type mitochondrial genome, while absence of restoration means that the mutant has no mitochondrial DNA. Therefore, the colonies that did not grow on glycerol or were sectored, were crossed with the IL166-6C rho$^0$ tester strain. This cross gave prototrophic diploids that were replicated on YG medium. Diploid growth on glycerol was either absent or slow, and a good correlation with the growth of the parental haploid colonies on glycerol was observed (Fig. 6*c,d*). These data suggest that the defect of growth on glycerol originates from the loss of mitochondrial DNA in D273ΔYdl120 deletants, reflecting instability of the mitochondrial DNA on glucose medium.

Respiration rates of the wild-type and D273ΔYdl120 strains grown in liquid YPD medium at 28 °C was measured; D273ΔYdl120 was found to be less than 10% of the wild type (Table 1).

## Discussion

As an initial step in assessing the expression pattern of *Frda*, we cloned the corresponding mouse cDNA. Its sequence corresponded to the complete coding region of *FRDA*[6], and the positions of the putative initiation codons are conserved between the two species. Recently, Carvajal *et al.*[9] suggested that the frataxin gene might represent an alternatively spliced domain of an upstream gene designated *STM7* in humans. The mouse cDNA contig described here is 1.1 kb long and is missing some sequences at both the 5′ and 3′ ends, as indicated by the absence of polyadenylation signal and poly(A) tail. However, we did not find the sequence of mouse frataxin exon 2 to be spliced to the mouse *STM7* gene, as reported for rare human transcripts[9]. *Frda* was found to be expressed as a major transcript of 1.2 kb, a size very similar to that of the human mRNA. The presence of a 1.2-kb transcript and the absence of sequences from the mouse *STM7* gene in the cDNA clones are consistent with the original formulation of frataxin gene structure[6].

*In situ* hybridization experiments demonstrate that frataxin transcripts are expressed both within and outside the developing nervous system. Expression in dorsal-root ganglia of the spinal cord

**Table 1 • Mitochondrial defects of the D273ΔYdl120 deletion strain**

| | Wild type | D273ΔYdl120 |
|---|---|---|
| Respiration | 150 ± 10 | 10 ± 3 |
| % rho$^-$ mutants: | | |
| 28 °C | 0.5 ± 0.2 | 24 ± 3 |
| 37 °C | 24 ± 6 | 99 ± 1 |

Sodium azide–sensitive respiration is expressed in μl $O_2 \times h^{-1} \times 10^6$ cells$^{-1}$. The respiration and percentage of rho$^-$ mutants in the cell population after growth at 28 °C and 37 °C were measured as described in Methods.

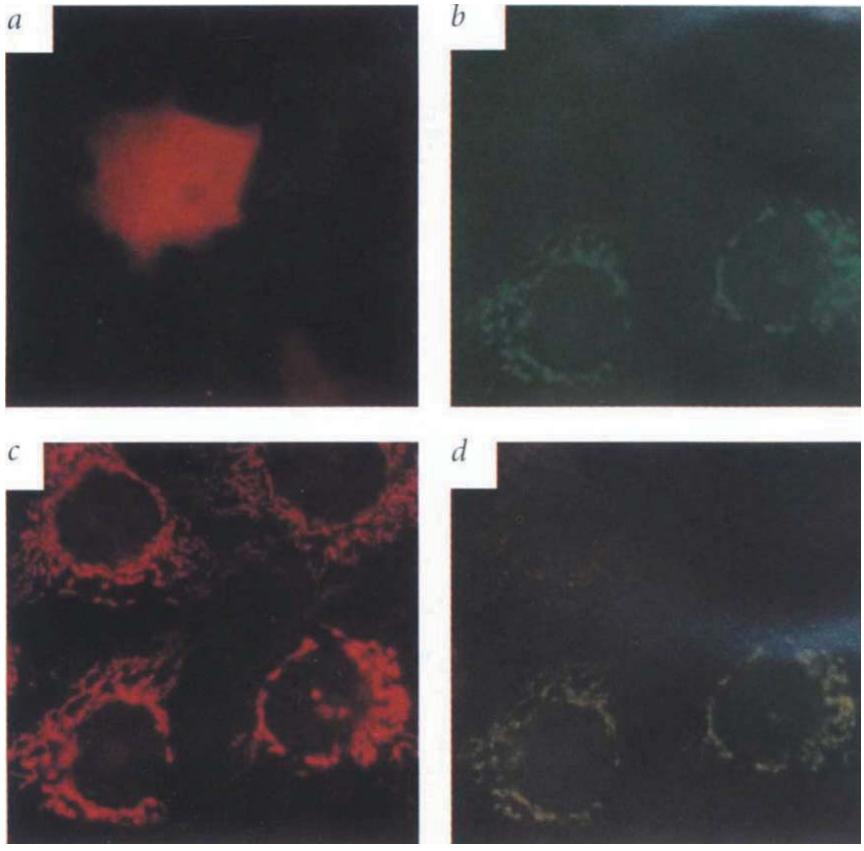


**Fig. 5** Mitochondrial localization of human frataxin. HeLa cells transfected with an expression vector for β-gal (*a*) or frataxin–β-gal fusion protein (*b–d*). ***a,*** Cells labelled with monoclonal anti–β-gal detected with Cy3 anti-mouse secondary antibody. ***b–d,*** Cells double-labelled with monoclonal anti–β-gal (detected with FITC anti-mouse secondary antibody) and anti-cytochrome-c oxidase antibody (detected with a Cy3 anti-rabbit secondary antibody). ***d,*** Co-localization of the two antibodies.

correlates with the principal site of neurodegeneration in FRDA that accounts for the loss of the large myelinated sensory fibres and neurodegeneration of the posterior columns. In contrast, degeneration of Clarke's columns and pyramidal and spinocerebellar tracts of the spinal cord[5] involves neurons in the posterior horn of the spinal cord and in the cerebral cortex that did not show expression above background level. This might therefore represent either post-synaptic or glial cell–induced degeneration, or a difference between human and mouse expression. The cerebellum of FRDA patients appears grossly normal when compared to the pathology seen in dominant ataxias and ataxia-telangiectasia[5]. However, faint hybridization signals within the cerebellar granule cell layer may correlate with clinical findings, such as nystagmus, that cannot be accounted for by spinal cord degeneration on its own.

It is of interest that some FRDA patients suffer from optic atrophy, which may relate to frataxin expression within the developing neural retina. *Frda* is also expressed in the embryonic and adult heart, which is consistent with human expression and correlates with the hypertrophic cardiomyopathy frequently seen in patients. Expression was found in several other tissues (such as the ventricular zone of the developing brain, brown fat, thymus) that appear unaffected in FRDA. This may indicate a lesser sensitivity of these tissues to frataxin deficiency or a difference in the level of expression between human and mouse, as in the case of adult kidney[6].

Our *in situ* data indicate that frataxin is predominantly expressed in tissues with a high rate of metabolism. Although liver, brown adipose tissue, heart and skeletal muscles differ in their use of fuels to meet energy needs[13], they are rich in mitochondria. These tissues, together with kidney and intestine, are typically affected in mitochondrial diseases[14]. Conservation of *FRDA*-like sequences in gram-negative bacteria but not in gram-positive bacteria led Gibson *et al.* to suggest that *FRDA* might result from the transfer of a

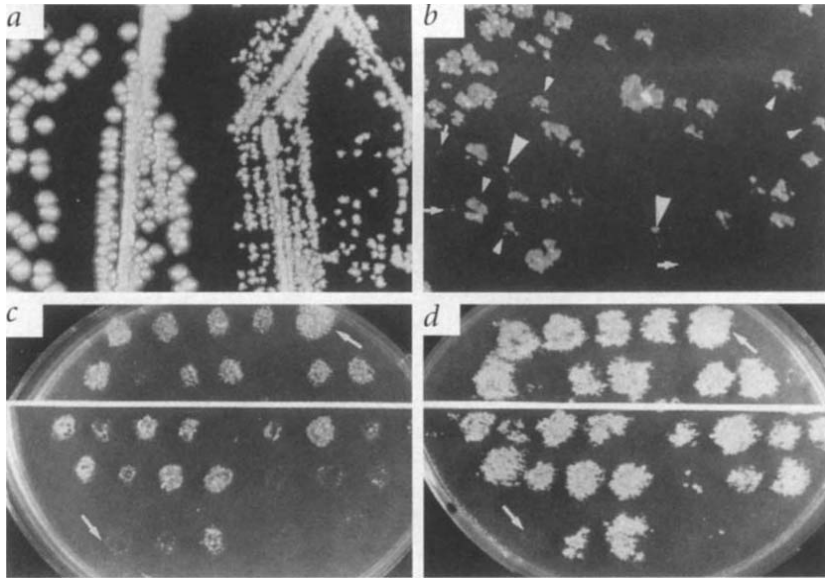


**Fig. 6** Glucose and glycerol growth defects of D273ΔYdl120. ***a,*** The wild-type strain D273UK (left) and deletion mutant D273ΔYdl120 (right) were streaked for single colonies on YPD plates and grown at 28 °C for 8 days. Note the small size and the scalloped shape of the mutant colonies. ***b,*** Colonies of D273ΔYdl120 grown on YPD medium were replicated on YG plates and grown at 28 °C for 2 days. Small arrow, small arrowhead and large arrowhead indicate colonies unable to grow on glycerol, sectored colonies and colonies giving rise to papillae, respectively. ***c,*** Colonies of D273ΔYdl120 grown and gridded on YPD medium were replicated on YG plates. Arrows indicate the position of a wild-type control (upper panel) and a rho$^0$ control (lower panel). ***d,*** The YPD grid used in experiment c was cross-replicated on a YPD lawn of the rho$^0$ tester strain IL166-6C; after 1 day at 28 °C, the mating plates were replicated on glucose minimum medium to select the diploids. The picture shows growth of the diploids after replica-plating on YG medium. Note that in most cases, growth of the diploids corresponding to crosses with glycerol-positive D273ΔYdl120 haploids is weaker than with the wild-type strain. It must also be noted that several haploid colonies that did not grow on glycerol gave rise to diploids exhibiting papillae, suggesting that a small fraction of the cells of these colonies still had mitochondrial DNA, which could be transmitted to the zygote and then correctly amplified in the presence of a wild-type *YFH1* allele; however, the number of mitochondrial DNA molecules present in the haploid deletant cells was probably too small to allow growth on glycerol.

gene from the endosymbiotic bacterial ancestor of the mitochondria to the nuclear genome[8] . Indeed, the N-terminal domain of the mouse and yeast frataxins contains a potential mitochondrial targeting sequence, corresponding to basic and hydroxylated residues along an amphiphilic α-helix[15].

The clear co-localization of tagged human frataxin with cytochrome-*c* oxidase, a well-known mitochondrial protein, indicates that the human frataxin also contains such a sequence, despite a lower fit with the consensus, and establishes frataxin as a mitochondrial protein encoded by the nuclear genome. The phenotype of yeast colonies with a disrupted *YFH1* gene supports a mitochondrial function for frataxin. When grown in glucose rich medium, frataxin deficient cells accumulate alterations, presumably mitochondrial DNA deletions, that make them unable to complement a strain devoid of mitochondrial DNA (rho$^0$). Oxygen consumption of these cells is also dramatically reduced. A mitochondrial function for frataxin has important implications for the understanding of the neurodegenerative process in FRDA.

Other neurodegenerative diseases are thought to involve oxidative stress that can lead to necrotic or apoptotic cell death[16]. Some forms of familial amyotrophic lateral sclerosis, a motor-neuron degenerative disease, are caused by mutations in the superoxide dismutase gene (SOD1)[17]. SOD1 catalyzes the formation of hydrogen peroxide from superoxide anions, and alterations of this cytosolic enzyme may result in mitochondrial degeneration in the motor neurons[18]. An FRDA-like phenotype occurs in ataxia with isolated vitamin E deficiency, which is caused by mutations in the α-tocopherol transfer protein[19], and vitamin E is known to inhibit lipid peroxidation by reactive free radicals[16]. Therefore, a plausible role for frataxin in mitochondria may be a direct or indirect protection against oxidative stress. Loss of this function in yeast defective for frataxin would lead to selection against mitochondrial function, accounting for the observed accumulating rho$^-$ mutants.

Note added in proof: The yeast *YSH1* gene was independently isolated by Babcock *et al*[20], as a multicopy suppressor of a mutant defective in low iron growth. Analysis of the *YSH1* disruptant, reported while this article was in press, similarly revealed a rho$^-$ phenotype and severe reduction in oxygen consumption. The authors also found a ten fold increase in mitochondrial iron, pointing to the likely cause of mitochondrial DNA deletion in the yeast disruptant and strengthening the hypothesis that frataxin deficiency results in oxidative stress, presumably as a result of iron-catalyzed Fenton chemistry.

## Methods

**Screening of a mouse cDNA library.** A total $2.7\times10^6$ individual clones of a mouse embryonic day-10.5 random-primed cDNA library (a gift of Dr. B. Galliot, Geneva) were screened with a PCR fragment of the human frataxin cDNA generated with primers TC 250: 5′–CTCTAGATGAGACCACCTATG–3′ and TG 162: 5′–TGAGCTCTGCGGCCAGCA–3′. Hybridization was performed as described by Sambrook *et al.*[21]. The filters were washed at 54 °C for 15 min in 2× SSC/0.1% SDS and 1× SSC/0.1% SDS.

**RNA isolation and northern blotting.** Total RNA was prepared from frozen adult mouse tissues (CD-1 background) according to the Trizol protocol (supplied by Gibco BRL, Grand Island, NE). Northern blots were prepared according to standard procedures[21]. Twenty micrograms of total RNA were loaded per lane. The probes, *mf1* and 36B4 (gift of Dr. E. Metzger, Strasbourg)[22], were labelled by the random priming procedure. The *mf1* probe had a $3\times10^9$ cpm/μg specific activity, and the northern blot was exposed for 10 days with intensifying screen.

***In situ* hybridization.** Embryos and fetuses from CD-1 mice were explanted from the uterus in phosphate-buffered saline (PBS). The relatively low level of expression of frataxin prevented the use of paraffin embedding, which is less sensitive than frozen sections. Embryos were frozen in OCT embedding medium and stored at –80 °C. Sections (10 μm thick) were performed with a cryostat set at –20 °C and collected on gelatinized slides. For all samples, series of consecutive sections were collected for hybridization with the antisense and sense probes (see below). The slides were treated before the hybridization as follows: They were dipped in acetone at 4 °C for 5 min and 4% formaldehyde in PBS at 4 °C for 15 min, rinsed in PBS twice for 5 min twice, immersed in 0.1M triethanolamine pH 8.0/0.25% acetic anhydride solution for 10 min, rinsed twice in 2× SSC for 2 min, incubated in 50% formamide/1× SSC at 60 °C for 10 min, dehydrated in increasing series of ethanol concentrations and air-dried.

The 548-bp *mf1* cDNA sub-cloned into the *Eco*RI site of Bluescript II SK+ (Stratagene, Palo Alto, CA) was used to prepare $^{35}$S-labelled riboprobes. The antisense and sense (control) probes were synthetized simultaneously in T3 and T7 *in vitro* transcription reactions, respectively, followed by partial alkaline hydrolysis to reduce the average probe length to about 150 nucleotides[22].

The *in situ* hybridization procedure was as described elsewhere[23]. After hybridization, the slides were washed twice in 1× SSC/50% formamide at 55 °C for 1 h, rinsed twice in 2× SSC for 5 min, treated with 20 mg/ml RNAse A and 1 U/ml RNAse T1 at 37 °C for 30 min, washed twice in 2× SSC/50% formamide at 55 °C for 1 h and in 0.1× SSC at 55 °C for 15 min, rinsed in water for 2 min and dehydrated. Slides were exposed under Kodak NTB-2 autoradiography emulsion for 4 to 5 weeks. All experiments included series of neighbouring sections hybridized to the antisense and control (sense) probes, and signals were considered specific when the control probe did not give labelling above background (as shown in Figs 3,4).

**Immunodetection of frataxin–β-gal fusion protein.** Human frataxin cDNA was amplified by PCR with flanking primers containing artificial *Kpn*I restriction sites (primers 5′–CCATGGTACCAAGTTCGAACCAACGTGGCCTC–3′ and 5′–GGCTGGTACCCAAGCATCTTTTCCGGAATAGGC–3′). The resulting PCR fragment was fused in frame via the *Kpn*I site to the sequence encoding β-galactosidase in pCHK vector[24], and proper fusion was confirmed by sequencing. HeLa cells were plated on Leighton tubes (Costar) and transfected with 1 μg/ml of plasmid DNA with calcium phosphate precipitation[25] for the transient expression of the constructs.

Forty hours after transfection, cells were fixed in 4% paraformaldehyde and permeabilized in 0.05% Triton X-100 (3× for 5 min). Cells were then incubated for 2 h at room temperature together with a monoclonal anti–β-gal antibody and a polyclonal antibody against cytochrome-*c* oxidase (gift of Dr. A. Lombès, INSERM U153, Paris). Revelation was carried out with FITC anti-mouse antibody and Cy3 anti-rabbit antibody (Jackson Lab).

**Yeast manipulations.** The following strain of *S. cerevisiae* was used: D273UK (*MAT alpha met6 ura3 lys2*). Yd1120w, which is the open reading frame of YFH1 and is located on chromosome IV (12), was deleted and replaced via homologous recombination[26] by a *kan*$^R$ marker containing cassette as described elsewhere[26]. The *YFH1* deletion starts at Ser$^{87}$ of the amino-acid sequence and encompasses the last amino-acid residue. The yeast strains were transformed and selected for resistance to geniticin G418, and the transformant clones were purified[27]. The correct insertion of the cassette was verified by PCR at the 5′ and 3′ extremities of the chromosomal deletion for 10 glycerol-positive and glycerol-negative transformants.

The cells were grown in 2% glucose (YPD medium) or 3% glycerol (YG medium), 1% yeast extract and 2% bactopeptone supplemented with 2% agar for solid media. The frequency of rho$^-$ mutants was evaluated by the number of colonies exhibiting a petite phenotype and failing to grow on glycerol. The rho$^-$ feature was verified by the absence of restoration of growth on glycerol in crosses with an rho$^0$ tester strain, IL166-6C (*MATa ura1*). The presence of complementary auxotrophies in D273UK and IL166-6C allowed selection of diploids on minimum medium. By definition, a rho$^-$ mutant (also called petite) has retained only small fragments of mitochondrial DNA or is completely devoid of mitochondrial DNA (rho$^0$).

Sodium azide–sensitive respiration was measured at 30 °C with a Clark electrode in a 3-ml vessel containing 2% glucose and 25 mM potassium phosphate, pH 6.5, at a cellular concentration of $200–300\times10^6$ cells per ml.

**Acknowledgements**

*We would like to thank M. Cossée and T.J. Gibson for discussions and sharing unpublished results; K. Fischbeck and J.-L. Mandel for suggestions and review of the manuscript; and S. Bronner, V. Fraulob, L. Reutenauer and B. Schuhbaur for their technical assistance. This work was supported by funds from the*

*Association Française contre les Myopathies (M.K.); CNRS, INSERM and the Ministère de l'Enseignement Supérieur et de la Recherche (M.K. and P.D.); the Services Fédéraux des Affaires Scientifiques, Techniques et Culturelles (PAI); and the Fond National de la Recherche Scientifique Belge (F.F.). H.K. is a recipient of a fellowship from the Association Française de l'Ataxie de Friedreich. V.C. is a recipient of the CEE fellowship.*

Received 4 December 1996; accepted 6 June 1997.

1. Skre, H. Friedreich's ataxia in western Norway. *Clin. Genet.* **7**, 287–298 (1975).
2. Romeo, G. *et al.* Incidence of Friedreich ataxia in Italy estimated from consanguineous marriages. *Am. J. Hum. Genet.* **35**, 523–529 (1983).
3. Harding, A. Friedreich's ataxia: a clinical and genetic study of 90 families with an analysis of early diagnostic criteria and intrafamilial clustering of clinical features. *Brain* **104**, 589–620 (1981).
4. Dürr, A. *et al.* Clinical and genetic abnormalities in patients with Friedreich's ataxia. *N. Engl. J. Med.* **335**, 1169–1175 (1996).
5. Oppenheimer, D.R. & Esiri, M.M. Disease of the basal ganglia, cerebellum and motor neurons. in *Greenfield's Neuropathology,* 5th ed. (eds Adams, J.H., Corselli, J.A.N. & Duchen, L.W.) 1015–1018 (Arnold, London, 1992).
6. Campuzano, V. *et al.* Friedreich ataxia, an autosomal recessive disease caused by intronic GAA triplet repeat expansion. *Science* **271**, 1423–1427 (1996).
7. Cossée, M. *et al.* Frataxin fracas. *Nature Genet.* **15**, 337 (1997).
8. Gibson, T.J., Koonin, E.V., Musco, G., Pastore, A. & Bork, P. Friedreich's ataxia protein: bacterial homologs point to mitochondrial dysfunction. *Trends Neurosci.* **19**, 465–468 (1996).
9. Carvajal, J.J. *et al.* The Friedreich's ataxia gene encodes a novel phosphatidyl inositol-4-phosphate 5-kinase. *Nature Genet.* **14**, 157–162 (1996).
10. Carvajal, J.J. *et al.* Friedreich's ataxia: a defect in signal transduction? *Hum. Mol. Genet.* **4**, 1411–1419 (1995).
11. Nakai, K. & Kanehisa, M. A knowledge base for predicting protein localization sites in eukaryotic cells. *Genomics* **14**, 897–911 (1992).
12. Goffeau, A. *et al.* Life with 6000 genes. *Science* **274**, 546–567 (1996).
13. Stryer, L. *Biochemistry* (W.H. Freeman & Co., New York, 1988).
14. Wallace, D.C., Shoffner, J.M., Trounce, I. & Brown, M.D. Mitochondrial DNA mutations in human degenerative diseases and aging. *Biochim. Biophys. Acta* **1271**, 141–151 (1995).
15. Schatz, G. & Dobberstein, B. Common principles of protein translocation across membranes. *Science* **271**, 1519–1526 (1996).
16. Halliwell, B. Free radicals, antioxidants, and human disease: curiosity, cause or consequence? *Lancet* **344**, 721–724 (1994).
17. Rosen, D.R. *et al.* Mutations in Cu/Zn superoxide dismutase gene are associated with familial amyotrophic lateral sclerosis. *Nature* **362**, 59–62 (1993).
18. Wong, P.C. *et al.* An adverse property of familial ALS-linked SOD1 mutation causes motor neuron disease characterized by vacuolar degeneration of mitochondria. *Neuron* **14**, 1105–1116 (1995).
19. Ouahchi, K. *et al.* Ataxia with isolated vitamin E deficiency is caused by mutations in the α-tocopherol transfer protein. *Nature Genet.* **9**, 141–145 (1995).
20. Babcock, M. *et al.* Regulation of mitochondrial iron accumulation by Yfh1p, a putative homolog of frataxin. *Science* **276**, 1709–1712 (1997).
21. Sambrook, J., Fritsch, E.F. & Maniatis,T. *Molecular Clonning: A Laboratory Manual* (Cold Spring Harbor Laboratory Press, Cold Spring Harbor, NY, 1989).
22. Krowczynska, A.M., Coutts, M., Makrides, S. & Brawerman, G. The mouse homologue of the human acidic ribosomal phosphoprotein PO: a highly conserved polypeptide that is under translational control. *Nucleic Acids Res.* **17**, 6408 (1989).
23. Décimo, D., Georges-Labousse, E. & Dollé, P. in *Gene Probes 2, a Practical Approach* (eds Hames, B.D. & Higgins, S.J.) 183–210 (IRL Press, Oxford, 1995).
24. Schreiber, V., de Murcia, G. & Murcia, J.M. An eucaryotic expression vector for the study of nuclear localization signals. *Gene* **150**, 411–412 (1996).
25. Gorman, C.M., Lane, D.P. & Rigby, P.W. High efficiency gene transfer into mammalian cells. *Philos. Trans. R. Soc. Lond. Biol. Sci.* **307**, 343–346 (1984).
26. Rothstein, R. Targeting, disruption, replacement, and allele rescue: integrative DNA transformation in yeast. *Methods Enzymol.* **194**, 281–301 (1991).
27. Wach, A., Brachat, A., Pöhlman, R. & Philipsen, P. New heterologous modules for classical or PCR-based gene disruptions in *Saccharomyces cerevisiae*. *Yeast* 10, 1793–1808 (1994).